Eur. Phys. J. D **6**, 327–332 (1999)

THE EUROPEAN PHYSICAL JOURNAL D

EDP Sciences

High-resolution measurements of line intensity, broadening and shift of CO_2 around 2 μm

C. Corsi[a], F. D'Amato[b], M. De Rosa[c], and G. Modugno[d]

INFM-Sezione di Firenze, and LENS-European Laboratory for Non-Linear Spectroscopy
Dipartimento di Fisica, Università di Firenze, Largo E. Fermi 2, 50125 Firenze, Italy

Received: 24 April 1998 / Received in final form: 28 October 1998

Abstract. Fundamental spectroscopical parameters of CO_2 are reported using a high resolution, direct absorption spectrometer, based on a distributed feed-back diode laser emitting at 2 μm. Line intensity, self- and foreign broadening and shift, with N_2 and O_2 as foreign gases, have been measured with high accuracy in the $\nu_1 + 2\nu_2^0 + \nu_3$ combination band of CO_2, for 13 lines of the R branch, from R(22) up to R(46). Comparison with available data is made, when possible, and a generally good agreement has been found.

PACS. 33.70.-w Intensities and shapes of molecular spectral lines and bands – 33.70.Jg Line and band widths, shapes, and shifts

1 Introduction

Carbon dioxide continues to stimulate even more and more interest to the spectroscopical community, for its relevant role in many areas of physics, chemistry, geology, etc.. The need of new and refined measurements of spectroscopical constants and lineshape parameters is of great importance for fundamental knowledge, such as the modeling of intermolecular potentials, and for many applications, such as sensitive detection of gas for environmental monitoring and medical diagnostics. A large amount of spectroscopical data are available for many bands of CO_2, mainly for intensities and broadenings [1-12], a little less for shifts [13-19]. Recently, spectrometers based on diode lasers emitting in the near infrared have been used for lineshape measurements in the $3\nu_3$ overtone band at 1.43 μm [17] and on the combination bands around 1.55 μm [18,19]. Particularly for the bands around 2 μm the available data have been obtained with Fourier Transform (FT) spectrometers with fairly good resolution [1,2,7], on the entire absorption bands. In the last years new semiconductor diode lasers have been developed to emit above 2 μm, based on material of III-IV groups. Tunable diode lasers have been shown to be suitable sources for high-resolution studies of transition lines. They have a high spectral purity, with emission linewidth below 10 MHz, which is at least one order of magnitude smaller than the best resolution of FT spectrometers. Moreover, they can be tuned continuously in a range of several wave numbers and easily swept across a single transition line, thus giving a detailed information on the lineshape.

Here we present the results of lineshape measurements over 13 lines of the $\nu_1 + 2\nu_2^0 + \nu_3$ combination band of CO_2 around 2μm, obtained with a newly developed distributed feed-back (DFB) diode laser. Line intensity, self- and foreign broadening and shift have been measured for all the lines and comparison with available data is made, when possible.

2 Experimental setup

A semiconductor diode laser has been used as laser source. It is an InGaAs/P DFB diode laser (Sensor Unlimited), driven by a low noise current source, while a temperature controller keeps its temperature stabilized within 0.001 K, and allows continuous, coarse tuning of the emitted wavelength, being the temperature tunability about 1.2 Å/°C. The fine tuning is made adjusting the value of the injection current, which typically runs between 70 and 100 mA. A current ramp is added too, in order to sweep a range of several GHz across a transition line.

The emitted radiation is collimated by a lens and after passing through an optical isolator (−35 dB) is divided in two beams: as shown in Figure 1, the first beam goes through the reference and sample cells, while the second

[a] *Current address*: Dipartimento di Scienze Neurologiche, Università di Firenze, Viale Morgagni 85, 50134 Firenze, Italy e-mail: `corsi@lens.unifi.it`

[b] *Current address*: ENEA, INN-FIS-SPET, Via E. Fermi 45, 00044 Frascati (RM), Italy

[c] *Current address*: SIT, Firenze, Italy

[d] *Current address*: Scuola Normale Superiore, Piazza dei Cavalieri 7, 56126 Pisa, Italy

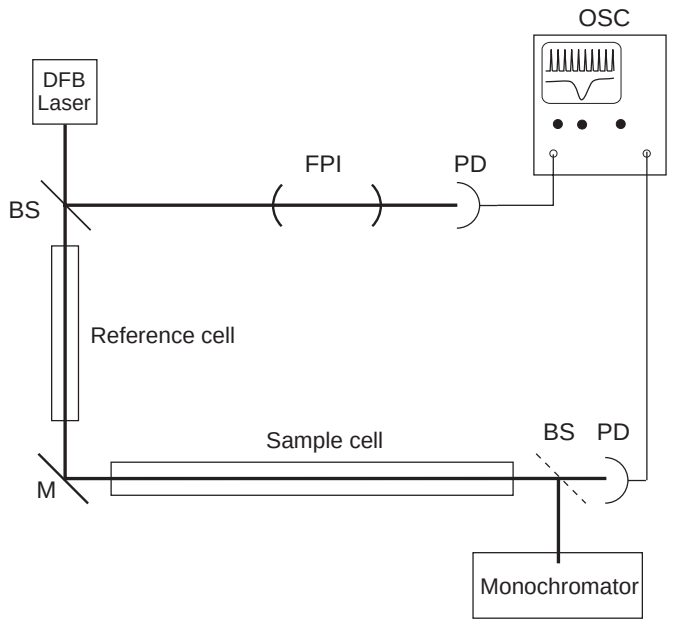

Fig. 1. Experimental setup for the measurement of broadening and shift; for linestrength measurements only one cell is present. BS: beam splitter; M: mirror; PD: photodetector; FPI: Fabry-Perot interferometer; OSC: oscilloscope.

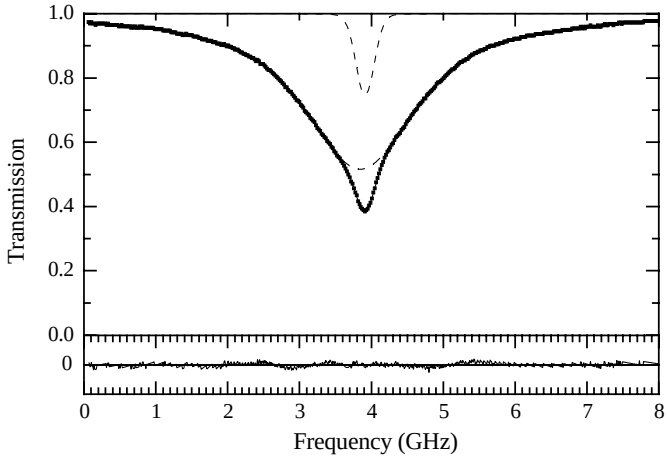

Fig. 2. An example of the fit for the transition R(24), perturbed by O_2 at a pressure of 300 Torr. The dashed lines correspond to the single deconvolved lineshape; at the bottom the residual is plotted magnified by 3.

one is sent through a 25 cm long confocal Fabry-Perot interferometer for the frequency scale determination. The measured free spectral range of the interferometer is 299 ± 1 MHz. Both beams are then collected by two InGaAs-PIN photodiodes (Hamamatsu, G5852-01). The signals from the photodetectors are acquired by a digital oscilloscope and then stored in a PC for the analysis.

For the measurements of the linestrengths a single cell has been used, while for broadening and shift measurements a two-cell arrangement has been used. The first cell is filled with few Torr of CO_2, and gives a reference peak for the measurement of shift, while the second cell is filled with CO_2 (and a foreign gas) at different pressures. Cells of different length, from 20 up to 150 cm, have been used in order to have the optimal signal resolution for different configurations and pressure ranges. The pressure has been monitored with two capacitive vacuum gauges (Varian), with a full scale of 10 Torr and 1000 Torr, respectively. With the help of a monochromator a preliminar map of the lines has been made in the frequency range covered by our diode laser, for the identification of the lines and of their quantum numbers.

The analysis of the data has been made with the help of the Linefit 2.0 software package [20]. The absorption signal is normalized with respect to the corresponding signal with empty cell(s), the frequency scale is linearized according to signal of the Fabry-Perot interferometer, then the absorption profile is fitted assuming Voigt profiles for the lineshapes. For broadening and shift measurements the absorption profile is the results of the overlap of two lineshapes coming from the two cells, Figure 2. For linestrength measurements the absorption profile is essentially Doppler broadened, with a small, but not negligible Lorentzian contribution. Fitting on purely Doppler broadened lineshape got a Gaussian half-width (HWHM) 142 ± 5 MHz, to be compared to the theoretical Doppler half-width 138 MHz, at $T = 23$ °C.

In some cases additional weaker lines, belonging to other bands of CO_2, are present in the vicinity of the investigated lines, which need to be included in the fit for a correct determination of the line parameters.

3 Results and discussion

The range covered by the diode laser includes 13 lines of the band $\nu_1 + 2\nu_2^0 + \nu_3$ of $^{12}CO_2$, from the R(22) up to R(46) lines. For all these lines we measured the intensity, the self- and foreign (with N_2 and O_2 as foreign gas) broadening and shift coefficients. Other weaker lines have been included in the fitting procedure, but the resulting lineshape parameters are not very reliable, with the exception, in few cases, of the broadening coefficients.

3.1 Line intensity

The radiation $I(\nu)$ transmitted through a gaseous sample is given by the Beer-Lambert law,

$$I(\nu) = I_0(\nu)\ \exp[-\alpha(\nu)\, L]\,, \tag{1}$$

where $I_0(\nu)$ is the intensity of the incoming radiation, $\alpha(\nu)$ is the absorption coefficient and L is the length of the optical path. The absorption coefficient $\alpha(\nu)$ can be written as

$$\alpha(\nu) = S\, N\, g(\nu - \nu_0)\,,$$

where S is the molecular line intensity, N is the concentration of the absorbing molecules, which is proportional to the pressure p, and $g(\nu - \nu_0)$ is the normalized lineshape function around the line center ν_0.

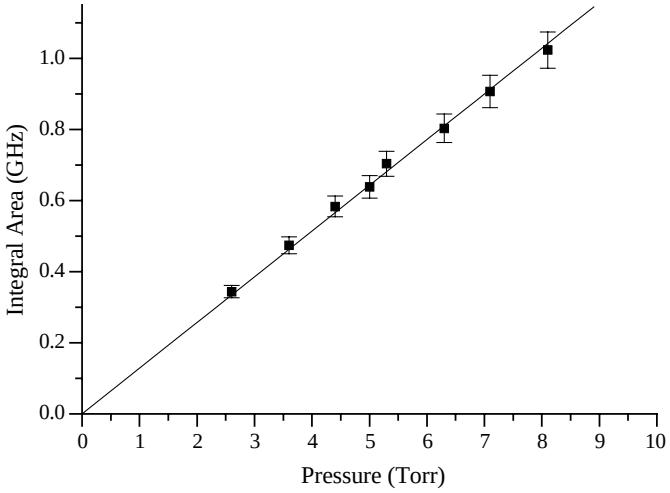

Fig. 3. Integral area of the absorption lineshape as a function of pressure for the line R(26): the cell was 151.5 cm long, the temperature was 23 °C.

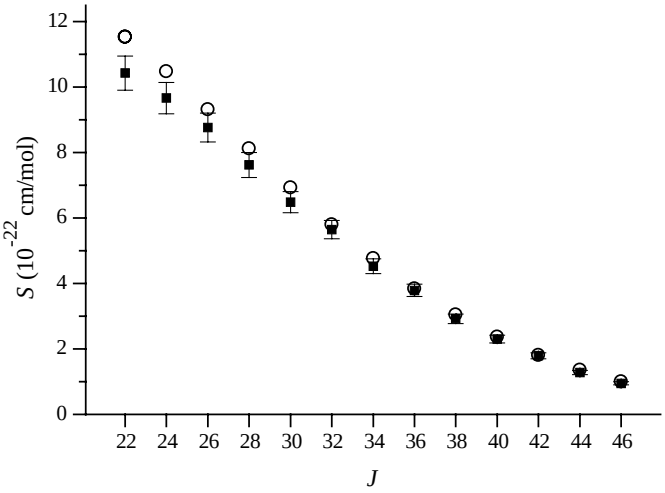

Fig. 4. Experimental line intensities (■), along with the corresponding values given by HITRAN database (○) are plotted *vs.* the rotational quantum number J.

A method [21] to determine the line intensity S is to extract from the experimental absorption profile the absorbance $\ln(I_0/I)$, according to equation (1) and integrate it numerically over the experimentally covered interval $\Delta\nu$, thus having

$$S = \frac{1}{L\,N}\int_{\Delta\nu} \ln(I_0/I)\,\mathrm{d}\nu\,.$$

Nevertheless this recipe could have two pitfalls. 1) The contribution of the wings of the profile could be understimate, due to the fact that a significative part, even if small, of the tails can be cutted away from the finite range swept around the line, moreover the finite resolution of the experimental signal together with the process of normalization mentioned above, can result in a net contribution to the integral. 2) In case two lines overlap, even poorly, it is impossible to separate the contribution to the absorption due to different lines. This was indeed the case of lines R(32), R(40) and R(46), which have small lines nearby. A different approach, which overcomes these difficulties, is to fit the absorption profile with a suitable number of lineshapes, and to build from the resulting lineshape parameters a synthetic, noise-free profile for every single line under investigation. Finally, each profile can be integrated over a sufficiently large interval.

Anyhow, we executed both the procedures, with the exception of the three, above-mentioned lines, and the results were equals, within the uncertainties. By repeating this procedure for profiles at different pressures we could further improve the accuracy. Hence, from a linear fitting of the integral area as a function of the pressure (Fig. 3), we obtained a value of the integral area per unit pressure, which was successively divided by the length L of the cell and by the number of molecules per unit volume, or Loschmidts' number $N_{\mathrm{L}}(T)$, at the temperature T of the gas. The error bars reported in Figure 3 are mainly determined by uncertainties on the normalization and on the pressure.

Table 1. Measured line intensity S and wave numbers ν_0 of the investigated lines of the $\nu_1 + 2\nu_2^0 + \nu_3$ band (R branch) of CO_2. The uncertainty reported is on the last significant digit. In the last column the data from HITRAN database are reported for a comparison.

J	ν_0[a] (cm^{-1})	S (10^{-22} cm/mol)	S_{H} (10^{-22} cm/mol)
22	4993.74361	10.4 (8)	11.53
24	4994.94121	9.7 (4)	10.48
26	4996.10895	8.8 (4)	9.32
28	4997.24681	7.6 (4)	8.12
30	4998.35475	6.5 (3)	6.93
32	4999.43277	5.6 (3)	5.80
34	5000.48083	4.5 (3)	4.77
36	5001.49895	3.8 (2)	3.84
38	5002.48710	2.9 (1)	3.04
40	5003.44529	2.3 (1)	2.37
42	5004.37352	1.7 (1)	1.81
44	5005.27182	1.28 (6)	1.36
46	5006.14021	0.95 (5)	1.00

[a] From HITRAN database

Two different cells have been used, with lengths 71.9 ± 0.2 cm and 151.5 ± 0.5 cm, respectively. The room temperature has been monitored to be stable during each series within 1 °C, even if it varied for different series from 20 °C up to 23 °C. However, for a correct comparison with available data, all the line intensities have been referred to $T = 296$ K. The errors on the length of the cells and on the temperature are well within 1%, anyhow the total error on the final value of S, as reported in Table 1, has been estimated to be within 5%, which keeps account of

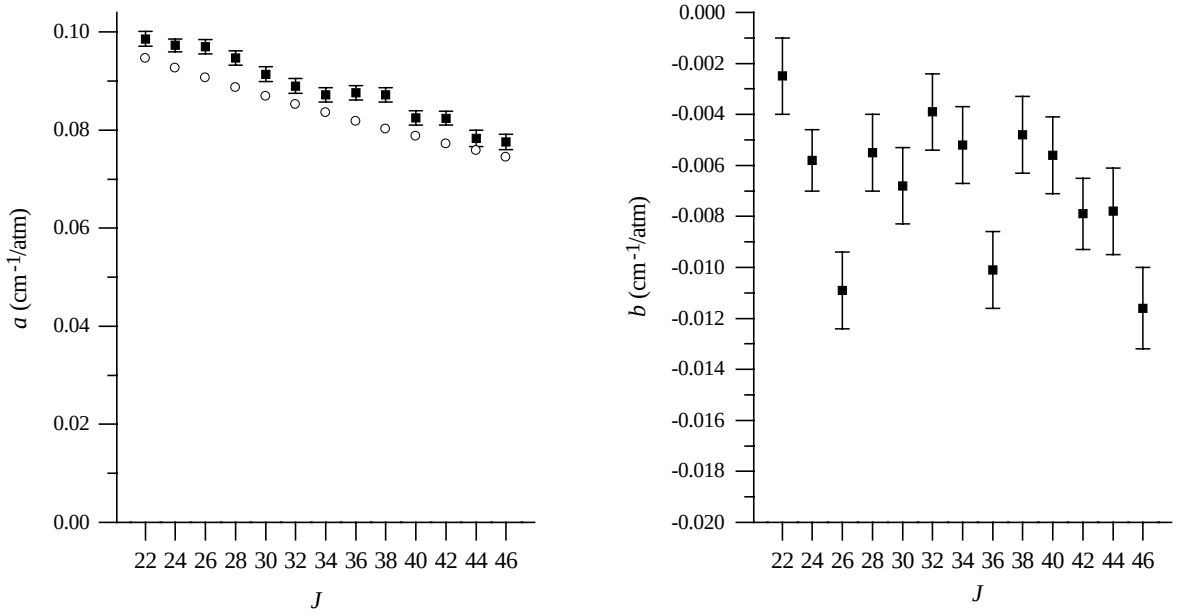

Fig. 5. Experimental self-induced broadening a (left) and shift b (right) coefficients are plotted *vs.* J; the values of self-broadening coefficients given by HITRAN (○) are also reported for comparison.

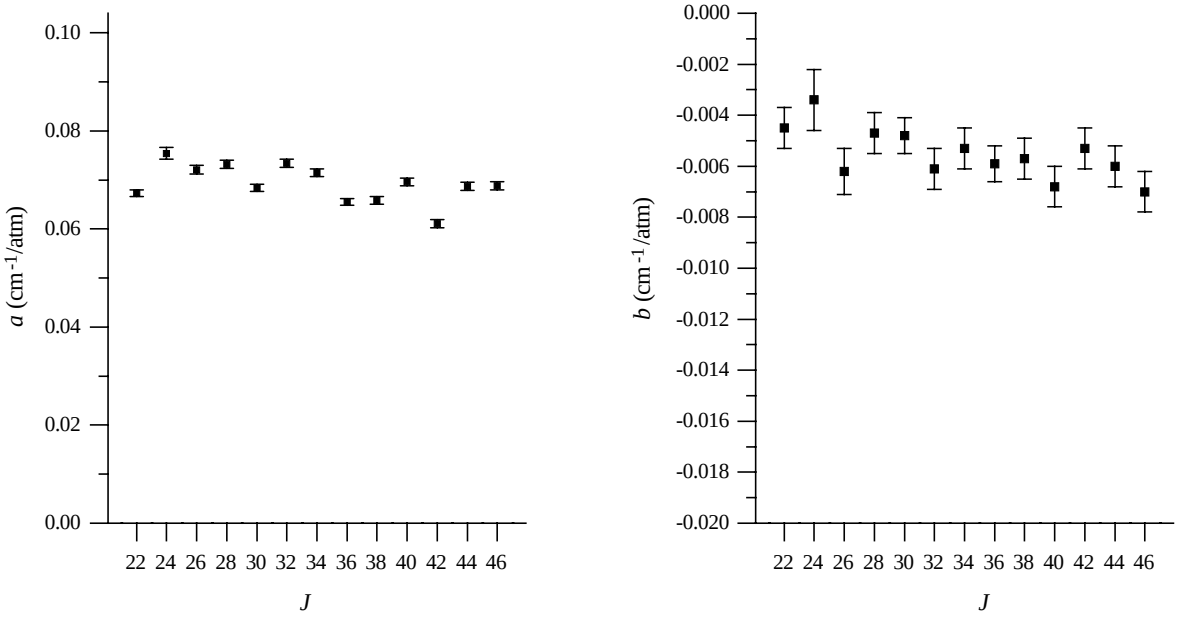

Fig. 6. Experimental N_2 induced broadening a (left) and shift b (right) coefficients are plotted *vs.* J.

the statistical spread and reproducibility of the result for different series. Line R(22) showed a larger spread and an error of 8% was assumed.

The resulting values of S are listed in Table 1, while in Figure 4 they are plotted along with the corresponding values from HITRAN database. Our values for S are sligthly smaller than HITRAN's ones, which have been measured with FT spectrometers [2,7], with a resolution which is at the best 0.004 cm^{-1}, *i.e.*, at least one order of magnitude worse than ours. When considering the errors reported the agreement with values in reference [7] is quite good.

3.2 Broadening and shift

In the case of pure CO_2 the Lorentzian half-width γ_L and the central position shift δ are assumed to vary linearly as a function of the pressure p,

$$\gamma_L = a_s\, p\,, \tag{2}$$

$$\delta = b_s\, p\,, \tag{3}$$

where a_s and b_s are the self-broadening and self-shift coefficients, respectively. If a buffer gas X is also present, then the effects will add together, according to the partial

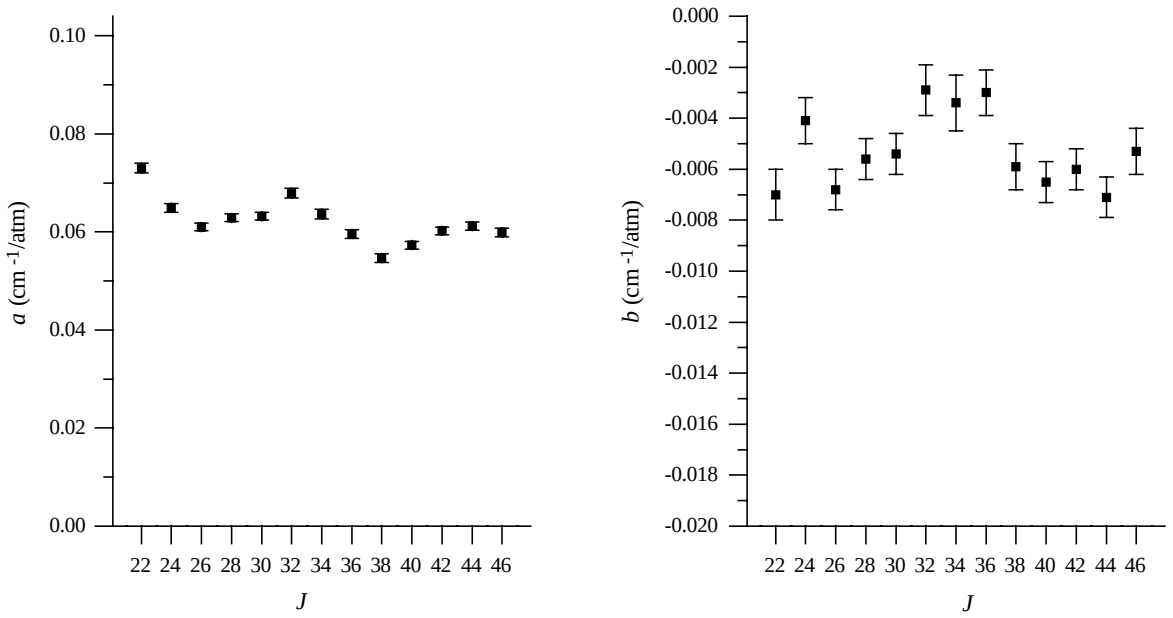

Fig. 7. Experimental O_2 induced broadening a (left) and shift b (right) coefficients are plotted *vs.* J.

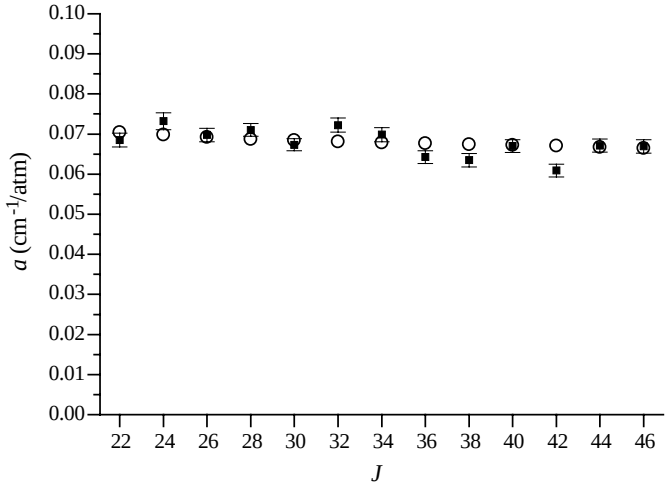

Fig. 8. Experimental air broadening coefficients a (■), as derived from equation (6), and corresponding data from HITRAN (○) are plotted *vs.* J.

pressures of the gases, as

$$\gamma_{\rm L} = a_{\rm s}\, p_{\rm CO_2} + a_{\rm X}\, p_{\rm X}\,, \tag{4}$$

$$\delta \;= b_{\rm s}\, p_{\rm CO_2} + b_{\rm X}\, p_{\rm X}\,, \tag{5}$$

where $a_{\rm X}$ and $b_{\rm X}$ are the foreign broadening and shift coefficients, $p_{\rm CO_2}$ and $p_{\rm X}$ are the partial pressure of CO_2 and of the perturbing gas X. So, we measured the Lorentzian half-width and the shift of the line center at different pressures; then we fitted them according to the laws of equations (2-5), in order to extract the coefficients a and b. The error for a single measure of the width and of the central position has been conservatively assumed to be 10 MHz, which is the spread of the Gaussian half-width retrieved from different absorptions at low pressure and reflects the total instrumental error. The errors for the broadening and shift coefficients are twice the standard deviation resulting from the linear fit of the data, according to equations (2-5). The result are summarized in Table 2 and in Figures 5-7.

The measured values for the self-broadening can be directly compared to the values given by HITRAN, Figure 5, while the air broadening coefficient can be derived from the values of N_2 and O_2 broadenings, according to

$$a_{\rm air} = 0.79\, a_{\rm N_2} + 0.21\, a_{\rm O_2}\,, \tag{6}$$

and compared, Figure 8, to the corresponding values reported by HITRAN.

The comparison with the data from HITRAN shows a good agreement, keeping in mind that HITRAN assumes the broadenings independent from the vibrational quantum numbers. This is a good approximation, which has been widely verified and justified theoretically [17], even if small differences appear when passing from one band to the other. Yet, HITRAN derives broadening coefficients by polynomial interpolation of available experimental data over different bands [11], so the dependence in the rotational quantum number J is smoothed out, while our experimental results show a more detailed picture of the J dependence. Previously experimental data, for the band here studied, were given for self- and N_2 induced broadening, with poor resolution (0.1 $\rm cm^{-1}$) [1], and a rough agreement (within 10%) is found for N_2, while substantial difference ($> 15\%$) is found for self broadening.

As far as the shifts are concerned, no previous data are available for the transitions here studied. Measurements on other bands show that pressure-induced shift has a marked dependence on the vibrational quantum number, the shift is always negative and typically increases when the vibrational numbers increase [17].

Table 2. Broadening a and shift b coefficients are listed for 13 lines of the $\nu_1 + 2\nu_2^0 + \nu_3$ band (R branch) of CO_2, for self-, N_2 and O_2 induced perturbation. The uncertainty on the last significant digit is twice the standard deviation.

J	Self		N_2		O_2	
	a (cm^{-1}/atm)	b (cm^{-1}/atm)	a (cm^{-1}/atm)	b (cm^{-1}/atm)	a (cm^{-1}/atm)	b (cm^{-1}/atm)
22	0.0986 (15)	−0.0025 (15)	0.0673 (7)	−0.0045 (8)	0.0730 (10)	−0.0070 (10)
24	0.0973 (13)	−0.0058 (12)	0.0754 (12)	−0.0034 (12)	0.0649 (9)	−0.0041 (9)
26	0.0970 (15)	−0.0109 (15)	0.0721 (9)	−0.0062 (9)	0.0610 (8)	−0.0068 (8)
28	0.0947 (15)	−0.0055 (15)	0.0732 (8)	−0.0047 (8)	0.0629 (8)	−0.0056 (8)
30	0.0914 (15)	−0.0068 (15)	0.0684 (7)	−0.0048 (7)	0.0632 (8)	−0.0054 (8)
32	0.0890 (15)	−0.0039 (15)	0.0734 (8)	−0.0061 (8)	0.0679 (10)	−0.0029 (10)
34	0.0872 (15)	−0.0052 (15)	0.0715 (8)	−0.0053 (8)	0.0636 (10)	−0.0034 (11)
36	0.0876 (15)	−0.0101 (15)	0.0655 (7)	−0.0059 (7)	0.0596 (9)	−0.0030 (9)
38	0.0872 (15)	−0.0048 (15)	0.0658 (8)	−0.0057 (8)	0.0547 (9)	−0.0059 (9)
40	0.0825 (15)	−0.0056 (15)	0.0696 (8)	−0.0068 (8)	0.0573 (8)	−0.0065 (8)
42	0.0824 (14)	−0.0079 (14)	0.0611 (8)	−0.0053 (8)	0.0602 (8)	−0.0060 (8)
44	0.0783 (17)	−0.0078 (17)	0.0687 (8)	−0.0060 (8)	0.0612 (8)	−0.0071 (8)
46	0.0776 (16)	−0.0116 (16)	0.0688 (8)	−0.0070 (8)	0.0599 (9)	−0.0053 (9)

4 Conclusion

By using a DFB diode laser, we measured fundamental spectroscopical parameters for 13 ro-vibrational transitions of the $\nu_1 + 2\nu_2^0 + \nu_3$ combination band of CO_2. Line intensities, broadening and shift coefficients (also in presence of N_2 or O_2 as foreign buffer gas) have been measured with a resolution (∼10 MHz) higher than that typical of FT spectrometers, which have been previously used to perform such kind of measurements in this band. A comparison has been made with previously measured values and data from HITRAN database, and a generally good agreement has been found. To our knowledge for the $\nu_1 + 2\nu_2^0 + \nu_3$ band here studied, the values for the shifts have not been reported before.

Many thanks are due to Prof. Massimo Inguscio for useful discussion and reading of the manuscript. This work has been performed in the frame of ECC contract ERBFMGECT950017.

References

1. K.P. Vasilevskii, L.E. Danilochkina, V.A. Kazbanov, Opt. Spectrosc. **38**, 499 (1975).
2. F.P.J. Valero, C.B. Suárez, R.B. Boese, J. Quant. Spectrosc. Radiat. Transfer, **23**, 337 (1980).
3. E. Arié, N. Lacome, Ph. Arcas, A. Levy, Appl. Opt. **25**, 2584 (1986).
4. J.W.C. Johns, J. Mol. Spectrosc. **125**, 442 (1987).
5. L. Rosenmann, M.Y. Perrin, J. Taine, J. Chem. Phys. **88**, 2995 (1988).
6. V. Dana, A. Valentin, A. Hamdouni, L.S. Rothman, Appl. Opt. **28**, 2562 (1989).
7. C.B. Suárez, F.P.J. Valero, J. Mol. Specrosc., **140**, 407 (1990).
8. M. Hammerich, L. Vildrik-Sørensen, H. de Vries, J. Henningsen, Appl. Phys. B **53**, 170 (1991).
9. V. Dana, J.-Y. Mandin, G. Guelachvili, Q. Kou, M. Morillon-Chapey, R.B. Watson, L.S. Rothman, J. Mol. Spectrosc. **152**, 328 (1992).
10. J.-Y. Mandin, V. Dana, M. Badaoui, G. Guelachvili, M. Morillon-Chapey, Q. Kou, J. Mol. Spectrosc. **155**, 393 (1992).
11. L.S. Rothman, R.L. Hawkins, R.B. Wattson, R.R. Gamache, J. Quant. Spectrosc. Radiat. Transfer, **48**, 537 (1992).
12. J.-Y. Mandin, V. Dana, M.-Y. Allout, L.Régalia, A. Barbe, J.-J. Plateaux, J. Mol. Spectrosc. **170**, 604 (1995).
13. Ph. Arcas, E. Arié, C. Boulet, J.P. Maillard, J. Chem. Phys. **73**, 5383 (1980).
14. B. Lavorel, G. Millot, R. Saint-Loup, H. Berger, L. Bonamy, J. Bonamy, D. Robert, J. Chem. Phys. **93**, 2176 (1990); *ibidem*, J. Chem. Phys. **93**, 2185 (1990).
15. Q. Kou, G. Guelachvili, J. Mol. Spectrosc. **148**, 324 (1991).
16. V. Malathy Devi, D.C. Benner, C.P. Rinsland, M.A.H. Smith, J. Quant. Spectrosc. Radiat. Transfer **48**, 581 (1992).
17. F. Thibault, J. Boissoles, R. Le Doucen, J.P. Bouanich, Ph. Arcas, C. Boulet, J. Chem. Phys., **96**, 4945 (1992).
18. R.M. Mihalcea, D.S. Baer, R.K. Hanson, Appl. Opt. **36**, 8745 (1997).
19. M. De Rosa, C. Corsi, M. Gabrysch, F. D'Amato, J. Quant. Spectrosc. Radiat. Transfer **61**, 97 (1998).
20. F. D'Amato A. Ciucci, ENEA Report, RT/INN/94/01 (1994).
21. M.A.H. Smith, C.P. Rinsland, B. Fridovich, K. Narahari Rao, in *Molecular Spectroscopy: Modern Research*, edited by K. Narahari Rao, Vol. III (Academic Press, Orlando, 1992) p. 111-248.